# Hydraulic stability and wave overtopping of Starbloc ® armored mound breakwaters

Iman Safari, Dominique Mouazé, François Ropert, Sylvain Haquin, Alexander Ezersky

# Hydraulic stability and wave overtopping of Starbloc® armored mound breakwaters

Iman Safari [a,*], Dominique Mouazé [b], François Ropert [c], Sylvain Haquin [d], Alexander Ezersky [b]

[a] ESITC Caen, 1 rue Pierre et Marie Curie, 14610 Epron, France
[b] Normandie Univ, UNICAEN, UNIROUEN, CNRS, M2C, 14000 Caen, France
[c] Cerema Eau Mer Fleuves, 60280, Margny-Lès-Compiègne, France
[d] LHEEA Lab, Ecole Centrale de Nantes, CNRS UMR 6598, Nantes, France

## 1. Introduction

Over the last decades, single-layer armour has become a classical solution in coastal structure construction. The Accropode® blocks have been widely used worldwide since 1980 as armour protection on breakwaters. The use of a single layer (mainly for economic reasons) and its high hydraulic stability are the main advantages of this type of compact armour unit (CIRIA, CUR, CETMEF, 2007; Dupray and Roberts, 2009). Increasing attention has been paid by researchers to study and improve armour concrete units with even higher performance.

The main objective is to propose ways of optimisation allowing a high hydraulic stability, thereby leading to low consumption of concrete and thus significant cost savings as well as reduction in concrete mass used and consequent reduction in embodied CO2. A high-performance block therefore implies a reduced concrete consumption. In the same way, the overtopping performance of the unit also needs to be quantified due to the critical influence of the height of the structure, which therefore affects wave transmission.

From a general point of view, strong interlocking between units leads to increased stability of the layer. On the other hand, increasing the strength of interlocking causes a reduction in permeability (favouring a higher run-up, overtopping and wave transmission). An artificial unit must resolve this contradiction between hydraulic stability and hydraulic response by offering an optimal compromise.

The wide variety of these protection blocks is related not only to their shape, but also the methods of placement which play a crucial role. Recently, a number of design guidelines based on research data have been published (CIRIA et al, 2007).

The Coastal Engineering Manual (USACE, 2002) summarizes some results of hydraulic performance tests for several structures from different sources. In parallel, the TAW report (TAW, 2002) has provided a guideline on wave run-up and overtopping based on model tests. More recently, a new manual on wave run-up and overtopping (EurOtop, 2007, 2016 (pre-released version)) has superseded the older guidelines. In this manual, the authors have collected data concerning the overtopping discharges and roughness coefficients for rock and various concrete armour layers for different types of structure (permeable or impermeable slopes).

As a part of the CLASH project, Bruce et al. (2009) have reanalyzed the influence of armour type on overtopping. Furthermore, they have

* Corresponding author. ESITC Caen, 1 rue Pierre et Marie Curie, 14610 Epron, France.
*E-mail address:* iman.safari@esitc-caen.fr (I. Safari).

examined the effects of the roughness factor on various concrete and rock armour layers. Wave run-up and reflection on a small-scale model with Ecopode armour layer was examined by Buccino et al. (2011). Moreover, Molines and Medina (2015) reanalyzed the CLASH datasets, and reported the importance of such parameters on the roughness factor ($\gamma_f$) including, armour porosity and overtopping estimator.

In case of very steep slopes and small relative freeboards, Victor and Troch (2012) and Van der Meer and Bruce (2014) proposed a new formula that modifies this given in the EurOtop (2007).

In general, the stability of the armor layer increases with the packing density, and is thus associated with a reduction in porosity (CIRIA et al, 2007). On the other hand, the reduction in porosity is unfavourable as regards hydraulic response (run-up, overtopping).

Furthermore, interlocking units used in a single layer (e.g. Accropode®, Core-loc® and Xbloc®) are placed in a random attitude with a defined packing density and using a placement grid that specifies the position in the plane of the unit's center of gravity (CIRIA et al, 2007). This random character of placement configurations can contribute to worsening the scatter of the stability measurements and the hydraulic block performances. However, with a random placement, the orientation of the blocks and also their interlocking on the armour layer at a large scale can be substantially different from conditions used as a reference for the tests carried out on scale models. This issue has been resolved by comparing repeatability tests (EurOtop, 2007).

Presumably, the main weakness of efficient blocks (e.g. Accropode® or Xbloc®) arises from the fatigue strength of the material of the blocks, which results from oscillations otherwise known as rocking. This mode of damage is thought to occur at an early stage on the armour layer and can take place even with quite moderate wave height (Burcharth and Liu, 1994; Dupray and Roberts, 2009; Guo et al., 2015). Blocks are liable to oscillate when they do not benefit from a satisfactory base or interlocking. Their configuration allows them move from one equilibrium position to another, as a result of low oscillating forces.

A new unit the ‘Starbloc’ has been developed as an endeavour to cope with the above mentioned difficulties.

Focusing on the complex armour unit with random placement in a single layer, it is logical to consider that the (expected) number of delicate equilibrium positions increases with the number of legs on a given block. Therefore, less force will be required to move the block from one equilibrium to another. To limit the risks of oscillation, the supports of the block need to be located as far away as possible from each other. This is one of the reasons it is adopted a block with 3 legs, which represents a straightforward choice.

Furthermore, a reduced number of legs means larger spaces between them, and therefore easier interlocking.

On the other hand, the leg size has to be substantial to ensure structural strength. Indeed, these bulky legs also allow an easy covering of one block upon another, which facilitates orderly placements.

Finally, a nose is set on each side of the block to ensure thickness of the layer. The nose height is determined to fulfil the self-stability criterion.

Starbloc®, as a bulky armour unit (Dupray and Roberts, 2009), is designed to meet the following main criteria:

- it can be placed in a single layer in a random arrangement as well as in an orderly placement;
- simplicity of placement on the slope;
- able to facilitate interlocking;
- high hydraulic stability and performance (expected $Ns\ (KD) \approx 3\ (20),\ \gamma_f \approx 0.46$), therefore low occurrence of rocking;
- self-stable under its dead weight on a 3V: 4H slope;

To make reliable predictions of the hydraulic responses of ‘Starbloc®’, it is conducted an extensive 2D experimental campaign on the hydraulic stability and hydraulic response of this unit. Until now, no tests have been performed under 3D wave conditions. After these preliminary trials, we intend to carry out complementary tests such as 3D model tests (roundhead and oblique waves), placement studies and drop tests.

The objectives of these tests (2D) were as follows:

- firstly, to examine hydraulic stability and damage progression of the unit,
- secondly, to measure hydraulic response (overtopping),
- thirdly, to compare our results with those relating to other units (e.g. Accropode® or Xbloc®).

## 2. Starbloc®

Fig. 1 shows the ‘Starbloc®’ unit. It is composed of a central core forming an irregular hexagonal, three ‘square leg’ extensions and two ‘noses’ of truncated pyramidal shape with a hexagonal base (Safari, 2011).

The ‘primary’ or ‘characteristic’ length can be used to normalize geometric dimensions. In the case of the Starbloc®, this dimension corresponds to the length of a side of a ‘square leg’, referred to here as the constant dimension ‘C’. Fig. 1 shows the dimensions, expressed in terms of ‘C’, and the different elements required to design the shape of the block.

The placement of the artificial blocks, after the construction of the core and the underlayer, can become a limiting factor for the progress of work. To determine the main parameters describing various arrangements, it is draw up 3D virtual views of the different proposed placement patterns.

In fact, the placement patterns are aimed at finding the best possible stability for:

- maximum interlocking of the blocks, taking into account their geometry, to avoid failure of the armour layer,
- optimal porosity of the armour layer to increase wave dissipation, in such a way that it minimizes the run-up as well as uplift pressure.

The packing density coefficient ($\phi$) and the porosity ($n_v$) is defined by

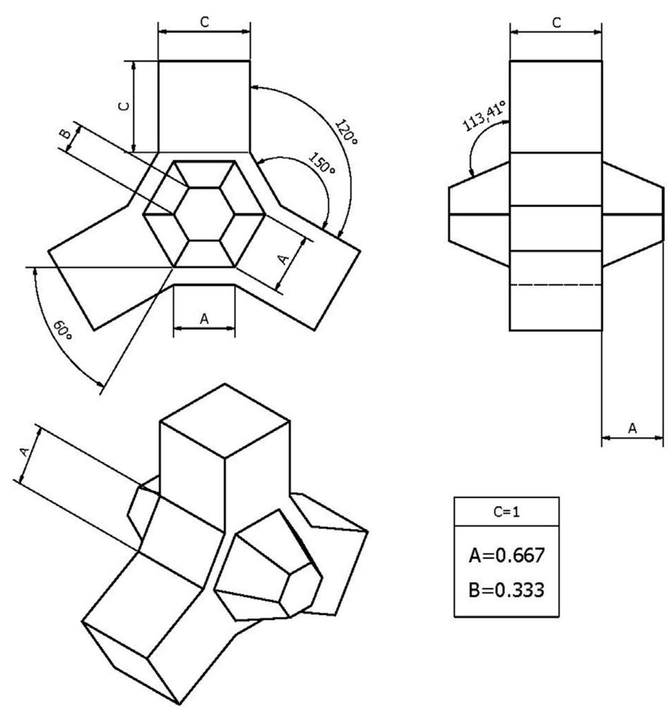


**Fig. 1.** 3D view of Starbloc® armour unit.


**Fig. 2.** Shipshape Placement pattern on 2-D model set-up.

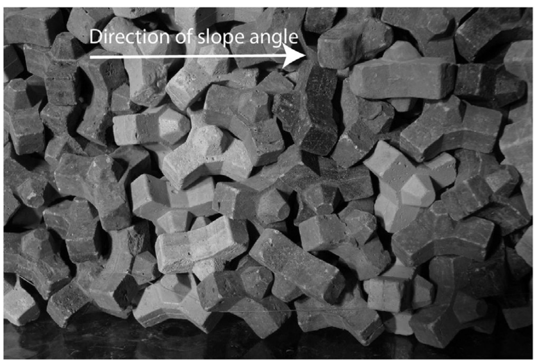


**Fig. 3.** Random Placement pattern on 2-D model set-up.

the following equation:

$$\phi = \frac{N}{A} D_n^2 = t_a(1 - n_v)/D_n \quad (1)$$

where N is the total number of units composing the armour, A the area units are covering, $D_n$ the nominal diameter, and $t_a$ armour layer thickness.

In the following sections, it is described two proposed placements for the Starbloc® units, 'Shipshape placement' and 'Random placement'. All the models are constructed in ideal conditions (perfect view, no water and construction by hand).

### 2.1. Shipshape placement

Fig. 2 shows the design placement pattern for the Starbloc® units used in one layer. It is assumed that the block is laid in two arrangements. In the first line, the blocks are arranged with the legs inclined at 45° to the line of greatest slope of the embankment. In fact, one leg points upward and two legs downward. In the second line, the blocks are placed between two lower blocks with the same angle. In this line, the direction of the legs is inverted, with one leg pointing downward and two legs upward. Thus, the configuration involves a covering of 2 legs by 2 legs. In this case, one of the upward pointing legs touches the nose of the lower block and the second leg touches one of the legs of the block on the left. Indeed, the nose of the lower block serves as a mark to place the notch of the upper block.

The blocks of the same horizontal line are placed in the same position. Evidently, there is an alternation of position between each line, with a "leg to bottom" block coming between two "leg to top" blocks.

The blocks have a three-point support on the filter, which is formed by a "nose" and the two legs, a triangle pointing to the top for the blocks placed "leg to top", and a triangle pointing downwards for the blocks placed "leg to bottom". Each block also has a two-point support on the underlying blocks. In this pattern, the horizontal and upslope distance were 1.6 $D_n$ and 0.98 $D_n$, respectively. Therefore, the packing density was $\phi = D_n^2/(1.6D_n{*}0.98D_n) = 0.64$.

### 2.2. Random placement

The blocks arranged in a random pattern are placed line by line, and do not follow any strict rule or specific positioning (Fig. 3). It may be considered this assembly as being 'natural', that is to say, the final placement that will be carried out most spontaneously under site conditions from a targeted sketched placement.

The main advantage of this placement is to obtain an armour layer that is as porous as possible while maintaining a sufficient interlocking to preserve stability.

The blocks are placed with various attitudes on the first line. Indeed, there is no control of the orientation and the blocks are placed in various positions deliberately, while avoiding adopting similar placements as the neighbouring blocks. This ensures that the blocks located on the first line are placed on three supports.

Then, the blocks are interlocked between two blocks of the line below. The placement attitudes of the blocks needs to be varied, with either the "leg" upward, or the "leg" downwards. In this pattern, the theoretical packing density was 0.60.

These configurations have insufficient strength to fully resist all the generated waves, and the results concerning the stability of this placement are discussed in the following paragraph.

## 3. Physical model tests

### 3.1. Experimental set-up

All the tests were carried out in the wave flume of the Coastal and Continental Morphodynamics laboratory of the University of Caen. The experimental tests were performed in a wave flume measuring 0.8 m wide, 22 m long, and 1.0 m high. The water depth was 0.455 m. This flume is equipped with an Edinburgh Designs piston wave generator that can generate regular and irregular waves with active wave reflection compensation (Edesign.co.uk, 2016). The sidewalls of the flume are made of glass, allowing clear observations and optical measurement of wave-model interactions (Fig. 4). All tests were conducted on flat bottom.

The sketch of the breakwater cross-section, as well as, material characteristics used in this model, are presented in Fig. 5. There are some methods to estimate scale effects on core permeability such as Burcharth

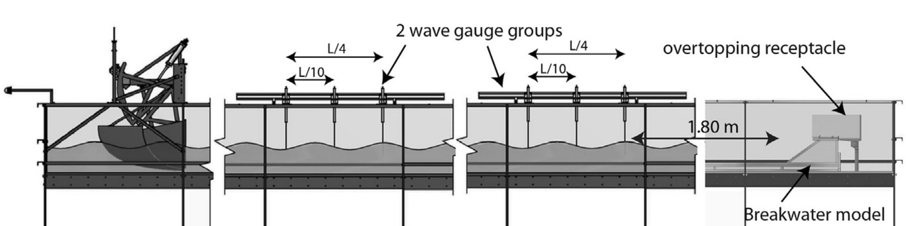


**Fig. 4.** Schematic diagram of wave flume and instrumentation.

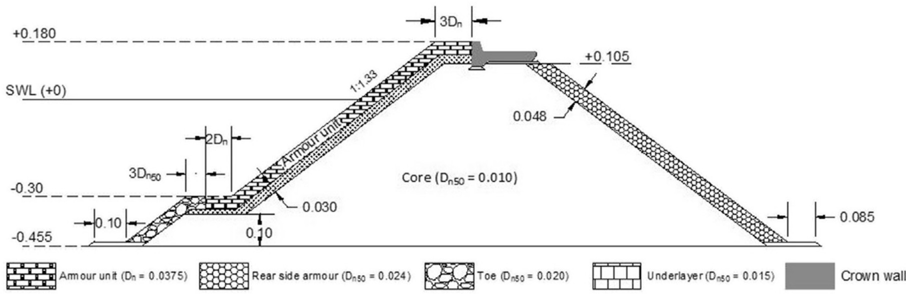


**Fig. 5.** Cross section of 2-D model set-up.

**Table 1**
Properties of unit and model parameters.

| Elements | $\rho_s$ [kg/m$^3$] | $D_{n50}$ [m] | $M_{50}$ [kg] |
|---|---|---|---|
| Armour layer | 1 620 | 0.0375 | 0.0850 |
| Under layer | 2 650 | 0.0160 | 0.0100 |
| Core | 2 650 | 0.0100 | 0.0026 |

et al. (1999), Vanneste and Troch (2012), and Wolters et al. (2014). In this study, the dimension of core materials has been determined according to the method proposed by Burcharth et al. (1999). Finally the core nominal diameter ($D_{n50}$) is calculated to 0.010 m. The underlayer is composed of stones ($M_{50}$ = 0.010 kg, $\rho$ = 2 650 kg/m$^3$) with a nominal diameter $D_{n50}$ = 0.015 m. The thickness of the underlayer was about $2D_{n50}$ = 0.030 m.

The dimensions of the model are limited by the capabilities of wave generation (significant wave height and period). The armour layer is built using 'Starbloc®' with a median mass of 0.085 kg, and a nominal diameter of 0.0375 m. It must be noted that the mean mass density of unit is exactly 1 620 kg/m$^3$, lower than the normal concrete elements (2 400 kg/m$^3$). The reason for this was that the dimensions of the model were limited by the capabilities of the wave generation (significant wave height and period), and nevertheless the major dominant forces are reproduced in correct proportion (Hughes, 1993) at the initiation of damages. This is relevant to estimate the armour stability. The same technique (light units of 1860 kg/m$^3$) has been validated and used successfully by Gómez-Martín and Medina (2006) to study a highly stable bloc (Cupipod).

The tests are carried out depending on wave parameters such as the wave height and wave period, as well as properties of the armour layer such as placement, packing density, freeboard, etc. The tests parameters are summarized in the following Table 1 and Table 2. The water depth at the toe of the slope was 0.455 m, the crown height Rc was 0.18 m (stability and overtopping tests) or 0.08 m (for some overtopping tests). The crown width was 3 rows of blocks.

### 3.2. Wave measurements

Two groups of three resistance-type wave gauges, with a precision of ±2%, are used to measure the water surface elevations in the flume. The first group is placed with some distance from the wave maker (10 m) while the second group is positioned 1.5 m seaward of the structure toe. Incident and reflected waves are resolved using the least-squares technique described by Mansard and Funke (1981).

Each test was performed with a target mean peak period and Iribarren's number, $\xi$, varied from test to test:

$$\xi = tan\alpha \Big/ (H_s/L_0)^{1/2} \tag{2}$$

where $H_s$ is the significant wave height at the toe of the structure and $L_0 = gT_p^2/2\pi$, $T_p$ is the peak wave period and $\alpha$ is the armour slope angle. Here, the significant wave height $H_{m0}$ (=$H_s$) and $T_p$ (peak wave period) are obtained from the frequency domain analysis.

Each series of tests starts with a low wave height resulting in no damage (packing test). Subsequently, the wave height is increased (with a fixed wave period) in increments up to a wave height resulting in unacceptable damage (failure). Therefore, each test series consisted of 3–6 runs with increasing wave height. $T_p$ being fixed and $H_s$ variable during each series, the Iribarren's number changes within the same series. This approach is therefore different from the one adopted in Medina et al. (2014), where the Iribarren's number was kept constant. All tests were conducted in non-breaking waves conditions (Table 2).

All tests are conducted using irregular waves using a JONSWAP spectrum ($\gamma$ = 3.3). The stability test for each wave height is performed

**Table 2**
Summary of hydraulic stability wave conditions.

| Test n. | Geometry | | | | | | | Wave conditions | | |
|---|---|---|---|---|---|---|---|---|---|---|
| | Placement pattern | N. of tests | $D_n$ (m) | Rc (m) | d (m) | $t_a$ (m) | $\phi$ | $T_p$ (s) | $H_{m0}$/d | $\xi_p$ |
| 1 | Shipshape | 5 | 0.375 | 0.18 | 0.45 | 0.060 | 0.64 | 1.73 | 0.184–0.291 | 4.4–5.6 |
| 2 | Shipshape | 5 | 0.375 | 0.18 | 0.45 | 0.060 | 0.64 | 1.73 | 0.185–0.289 | 4.4–5.6 |
| 3 | Shipshape | 6 | 0.375 | 0.18 | 0.45 | 0.060 | 0.64 | 1.96 | 0.121–0.290 | 5.1–7.9 |
| 4 | Shipshape | 5 | 0.375 | 0.18 | 0.45 | 0.060 | 0.64 | 1.25 | 0.178–0.271 | 3.3–4.1 |
| 5 | Shipshape | 5 | 0.375 | 0.18 | 0.45 | 0.060 | 0.64 | 1.73 | 0.092–0.293 | 4.5–7.9 |
| 6 | Shipshape | 7 | 0.375 | 0.18 | 0.45 | 0.060 | 0.64 | 1.52 | 0.117–0.287 | 3.7–6.2 |
| 7 | Shipshape | 6 | 0.375 | 0.18 | 0.45 | 0.060 | 0.64 | 1.25 | 0.176–0.270 | 3.3–4.0 |
| 8 | Shipshape | 5 | 0.375 | 0.18 | 0.45 | 0.060 | 0.64 | 1.72 | 0.164–0.264 | 4.6–5.2 |
| 9 | Random | 5 | 0.375 | 0.18 | 0.45 | 0.057 | 0.60 | 1.73 | 0.123–0.213 | 5.2–6.9 |
| 10 | Random | 5 | 0.375 | 0.18 | 0.45 | 0.057 | 0.60 | 1.73 | 0.126–0.187 | 5.6–6.8 |
| 11 | Random | 5 | 0.375 | 0.18 | 0.45 | 0.057 | 0.60 | 1.52 | 0.120–0.192 | 4.8–6.2 |
| 12 | Random | 4 | 0.375 | 0.18 | 0.45 | 0.057 | 0.60 | 1.52 | 0.120–0.166 | 5.2–6.2 |
| 13 | Random | 5 | 0.375 | 0.18 | 0.45 | 0.057 | 0.60 | 1.52 | 0.093–0.178 | 5.1–7.0 |
| 14 | Shipshape | 4 | 0.375 | 0.18 | 0.45 | 0.060 | 0.72 | 1.52 | 0.071–0.119 | 6.2–8.0 |
| 15 | Shipshape | 4 | 0.375 | 0.18 | 0.45 | 0.060 | 0.72 | 1.52 | 0.071–0.120 | 6.1–7.9 |

Note: d: water depth; $t_a$: armour unit thickness; $\phi$: packing density; $T_p$: peak wave period; $H_{m0}$: significant wave height (frequency domain analysis); $\xi_p$: Iribarren number for peak wave period.

for fixed acquisition duration, from 1 024 s to 2048 s. This corresponds to 1 000 to 1700 waves depending on the tested wave period. Wave statistic significance is already achieved for 1 000 waves. The measurement data are obtained using a sample frequency of 32 Hz. In order to obtain the accurate generations of wave, all wave conditions were calibrated through a transfer function with the model in place. Before starting each test, the wave gauges were calibrated in still water through three fixed positions (+0.025 m, 0 m, −0.025 m).

### 3.3. Experimental measurements

#### 3.3.1. Measurement of damage

Armour damage measurements in this study are obtained by visual observations of the displacements of the blocks of the armour layer. To improve visualization of displacement and the orientation change of the blocks during damage, the blocks are placed in different coloured strips.

Photographs of the armour layer are taken after each series of tests to measure the evolution of the damage (before, during and after the test). Conventionally, two different levels of damage were considered in this study. First of all, start of damage is defined by any movement (rocking to departure) or the extraction of a block from its initial position. Finally, with increasing wave height, the failure of the armour layer is reached when removal of a number of blocks leads to the exposure of the filter layer or the core. Damages were not repaired during succeeding test series. In this way the cumulative damage during the test series was determined. The armour layer is reconstructed if necessary, only after completion of each test series.

The experimental results shown in Fig. 6 highlight the evolution of damage. In this figure, the results are presented in terms of the dimensionless parameters used, such as the stability number $N_s$ (Van der Meer, 1999), against the Iribarren number ($\xi_p$):

$$N_s = \frac{H_s}{\Delta D_n} = (K_D \cot \alpha)^{1/3} \tag{3}$$

where $N_s$ = stability number;

$K_D$ = stability coefficient (introduced by Hudson (1959));
$H_{m0} = H_s$ = significant wave height in front of the structure; $\Delta = (\rho a/\rho w\text{-}1)$;
$\rho_a$ = mass density of the armour unit;
$\rho_w$ = mass density of the water;
$D_n$ = nominal diameter of the unit = $(m/\rho_a)^{1/3}$;
m = mass of the armour unit;
$\alpha$ = slope angle.

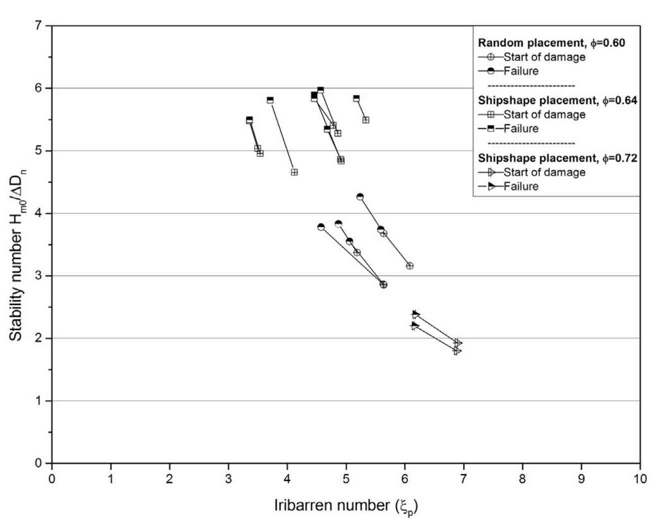


**Fig. 6.** Influence of placement pattern and porosity on stability.

#### 3.3.2. Overtopping measurement

The overtopping response to different parameters such as slope geometry or crest level (presence of a crown wall) has been examined in various model investigations (Bradbury et al., 1988; Owen, 1980; Van der Meer and Stam, 1992; Aminti and Franco, 1988; Van Gent et al., 2007; Bruce et al., 2009; Molines and Medina, 2015).

In this study, the mean overtopping rate is measured for all tests, using the same standard method described by researchers such as Möller et al. (2003). The overtopping discharge ($m^3/s/m$) is measured here using a receptacle located behind the breakwater model as shown in Fig. 4. This container consists of 10-mm-thick PVC plates, with dimensions of 0.795 m × 0.785 m x 0.360 m (length x width x height).

The data analysis allows us to calculate the average overtopping rate, i.e. the quantity of water collected in the receptacle during a sequence of N incident waves (a storm or period considered), per unit length of breakwater's width.

For this purpose, the discharge, q, is calculated according to the following formula:

$$q = \frac{V}{tB} \tag{4}$$

where

q: mean overtopping discharge;
V: accumulated wave overtopping volume;
t: test duration;
B: width of wave flume.

For tests with high overtopping rates, water is pumped into the leeward part of the wave flume during the test run to maintain a constant level of water in the front of the structure.

The accuracy of overtopping measurement is

- a receptacle with an uncertainty of 1.3% (calibration with given input water volumes),
- a chronometer with an operational accuracy precision of 1 s,
- a digital scale balance with an accuracy of 5 g (test weights),
- wave gauges with a precision of 2% (calibration in still water).

## 4. Test results

### 4.1. Armour hydraulic stability

Among the great variety of factors affecting the design of a breakwater, hydraulic stability appears to be one of the key design criteria that should be carefully examined, particularly in one-layer system. The geometry parameters and wave conditions are given in Table 2.

The graph presented in Fig. 6 represents values of the stability number ($N_s$) versus the Iribarren number $\xi_p$, for two placement examined. These tests were repeated at least two times in order to assess the actual reliability of the test results. The experimental packing densities were 0.64 and 0.60 for 'Shipshape' and 'Random' placement, respectively. The square symbols represent the stability numbers related to "Shipshape" placement, the circle symbols according to "Random" placement. Cross-center symbols correspond to the beginning of damage and the semi-full symbols show rupture of the armour layer. Here, as randomly placed armour units in a single layer, the initiation of damage corresponds to a standard designation of 'no damage' (CIRIA et al, 2007).

Fig. 6 shows that 'Starbloc®' units arranged in a "shipshape placement" with packing density 0.64 leads to a very high stability of the structure in contrast to random placement. However, results of shipshape placement with larger packing density ($\phi = 0.72$) will be discussed later.

In contrast to the behaviour observed with the shipshape arrangement, randomly placed blocks appear to perform poorly in terms of hydraulic stability. Moderate wave height is sufficient to extract one or more blocks, so the interlocking between units is drastically reduced. It is striking that the stability number remains rather low, at around 3.0, close to expected values found for comparable units such as 'Accropode®' or 'Xbloc®'(Van der Meer, 1999; CIRIA et al, 2007).

#### 4.1.1. *Influence of packing density*

The results are also presented in Fig. 6. The results show a considerable reduction of stability in the cases with highest packing density (0.72). This result is similar with those on the cube armour unit placed in a single and double layer given by Van Buchem (2009) and Vandenbosch et al. (2002).

However, the works of Vandenbosch et al. (2002) realized on tetrapod and Medina et al. (2014) with double layer randomly placed cubes show that increasing packing density induces an increasing of stability.

This discrepancy seems to be related to underpressure resulting from a permeability barrier inside the armour layer under specific conditions of placement (high packing density). This has been also pointed out by Van Buchem (2009) in the case of regularly placed cube for low porosity (20%). These interesting observations are examined further below in the discussion section.

It was also observed that the failure of the structure develops rapidly after the appearance of damage. This behaviour is explained by the fact that the wave height is sufficient to pull out one or more blocks, and interlocking is drastically decreased. At this point, the damage is highly concentrated, which leads to the formation of a large cavity in the armour layer. The underlayer is then exposed to the wave action, resulting in loss of underlayer materials.

#### 4.1.2. *Discussion*

Regarding the mechanism, the occurrence of damage starts on an 'active' area. This latter corresponds to a section extending from the middle of the breakwater crest down to a depth equivalent to the zero-damage wave height below still water level (CERC, 1984).

The blocks are destabilized by the combination of successive wave trains and extracted finally towards the toe during the run-down phase. At this point, the damage is strongly localized. This leads to large voids between individual blocks. The underlayer is then exposed directly to wave attack, causing loss of material. These observed damage processes indicate that a sequence of waves (of "moderate" wave height) can be more unfavourable than a solitary extreme wave.

It was noticed the shipshape placement looks more interlocked compared to random placement. Indeed, this highly interlocked armour layer reduces the risk of settlement of armour layer. In the case of shipshape placement, settlement of the armour unit is observed just after the start of damage. Nevertheless, some settlement has been observed for random placement before the start of damage. This settlement causes a decrease of packing density in the upper part of the armour layer and an increase in the lower part of the armour layer (Gómez-Martín and Medina, 2006).

With random placement, the inevitable movements of armour units and placement damage lead to arrangements where some blocks do not benefit from the expected interlocking between units, particularly those blocks placed on the critical zone. This explains why it is looked for a more efficient configuration, such as a 'Shipshape' placement, where the blocks are interlocked against each other.

The experimental values for the start of damage and failure found in model tests (CIRIA et al, 2007) can be described by the following equations, respectively:

$$N_s = \frac{H_s}{\Delta D_n} = 4.5 \quad \textit{start of damage}, \phi = 0.64 \tag{5}$$

$$N_s = \frac{H_s}{\Delta D_n} = 5.4 \quad \textit{failure}\ , \ \phi = 0.64 \tag{6}$$

**Table 3**
Summary of overtopping test conditions.

| Test | Slope angle | No. of tests | $T_p$ (s) | $H_{m0}/d$ | Rc (m) | ø |
|---|---|---|---|---|---|---|
| 1 | 2V:3H | 4 | 1.00 | 0.133–0.194 | 0.08 | 0.62 |
| | 3V:4H | 10 | | | | |
| 2 | 2V:3H | 4 | 1.20 | 0.141–0.27 | 0.08 | 0.63 |
| | 3V:4H | 17 | | | 0.18 | |
| 3 | 3V:4H | 9 | 1.50 | 0.114–0.228 | 0.18 | 0.62 |
| 4 | 3V:4H | 7 | 1.72 | 0.153–0.278 | 0.18 | 0.62 |

It must be noted these equations are related to a shipshape placement with a packing density of 0.64 and 3.5 < ξp < 5.5. For packing density of 0.72, the Ns is more lower than these values (Ns = 1.8–2.3).

As these values are close to other single armour unit such as Accropode ($N_s = 3.7$) or Coreloc ($N_s = 4.2$), it is recommended to use a safety factor of 1.5 on the ($H_s/\Delta D_n$) (CIRIA et al, 2007). Furthermore, the damage progresses quickly towards the failure of the armour layer, start of damage would be considered as the design stability criteria. Therefore the following equation could be used as design rule of 'Starbloc' unit:

$$\frac{H_s}{\Delta D_n} = 2.9\ (K_d = 18) \quad \textit{for design} \tag{7}$$

### 4.2. *Analysis of wave overtopping*

The previous section describes the method used in experimental tests to examine the effect of the shape of the new armour layer on overtopping. The amount of water discharge overtopping the crest structure is sampled per unit time and length of the breakwater.

In total 51 tests were carried out on a structure armoured with 'Starbloc' arranged in a shipshape pattern (Table 3). Two slopes are tested: 2V: 3H and 3V: 4H. The packing density is 0.64. Two water level are tested resulting in $R_c = 0.08$ m and 0.18 m (with $R_c$ the freeboard defined by the distance of the crest relative to still water level).

The influence of the conventional dimensionless crest freeboard on overtopping discharge is shown in Fig. 7, for two levels $R_c = 0.08$ m and $R_c = 0.18$ m. The dimensionless overtopping discharge is reduced by a factor of 10 when there is a 40% decrease in crest freeboard.

Fig. 7 show furthermore the influence of wave height and wave period on overtopping discharge. It can be seen that overtopping discharges are reduced slightly with decreasing wave period (almost by a factor 2). The crest of the wave becomes much steeper as the wave period decreases (increasing of wave steepness). Under this condition, there are two distinct effects and consequences. If the waves break before reaching the breakwater, they lose much of their energy and this results in a small run-up and hence reduced discharge. By contrast, if the waves break on

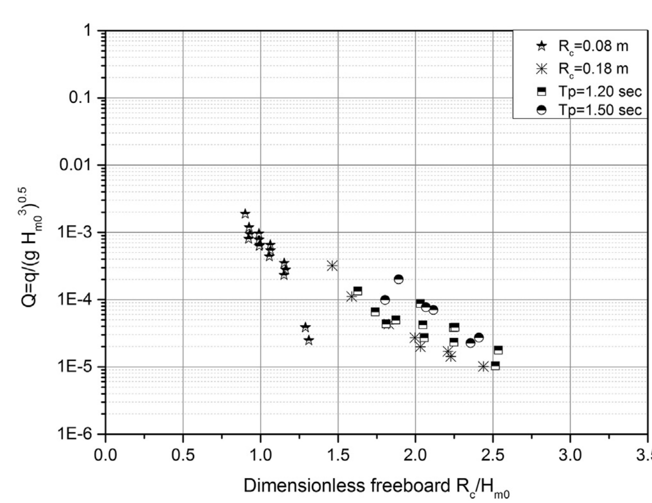


**Fig. 7.** Relative mean overtopping discharges against the relative freeboard.

**Table 4**
Roughness coefficients for single placed armour layer, from synthesis of new data and other comparable tests (Bruce et al., 2009).

| Type of armour | No. of layers | Slope angle | $\gamma_f$ Mean | $\gamma_f$ 95% CI, low | $\gamma_f$ 95% CI, high |
|---|---|---|---|---|---|
| Smooth | – | 1.5 | 1 | | |
| Rock (permeable core) | 1 | 1.5 | 0.45 | | |
| Cube | 1 | 1.5 | 0.49 | 0.46 | 0.52 |
| Accropode | 1 | 1.5 | 0.46 | 0.43 | 0.48 |
| Xbloc | 1 | 1.5 | 0.44 | 0.41 | 0.49 |
| Core-Loc | 1 | 1.5 | 0.44 | 0.41 | 0.47 |
| Starbloc | 1 | 1.33 | 0.40 | 0.38 | 0.43 |
| Starbloc | 1 | 1.5 | 0.45 | 0.43 | 0.47 |

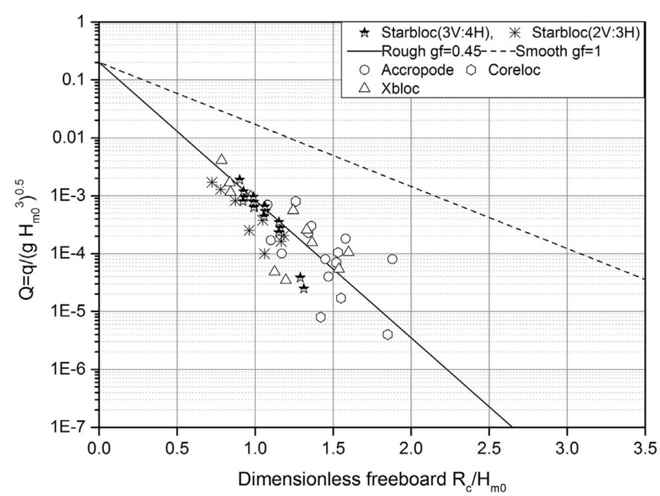


**Fig. 8.** Comparison of results of 'Starbloc' (Rc = 8 cm) with 'Accropode®', 'Coreloc®', 'Xbloc®' (Bruce et al., 2009).

the armour layer, they give rise to water jets or fluid projections that can accentuate the overtopping. This result is consistent with the work of Smolka et al. (2009) described by Molines and Medina (2015).

*4.2.1. Comparison with other single layer units*

The test profile is similar, particularly in regards to the crest of the structure (small freeboard), to those used in the tests carried out under the CLASH program and whose purpose was to provide roughness coefficients for natural stones and various types of artificial blocks (Bruce et al., 2009). These results serve as a reference Van der Meer and Janssen (1994) provided the initial overtopping formula, in case of non-breaking waves ($\xi_{m-1,0} > \approx 2$):

$$Q = q \Big/ \sqrt{gH_{m0}^3} = 0.2\exp\left(-2.6\frac{R_c}{H_{m0}}\frac{1}{\gamma_r}\right) \quad (8)$$

where q is the average specific overtopping discharge, $R_c$ the elevation of crest above SWL (m), $H_{m0}$ the spectral significant wave height at the toe of the structure, and $\gamma_r$ the roughness coefficient of the armour unit. Table 4 gives some recent roughness coefficients for single armour units, extracted from the CLASH programme (Bruce et al., 2009). It is also worth to remind that these results are referred to a structure with a slope 2V: 3H.

Fig. 8 shows a comparison of our results with those of other laboratories. To ensure a relevant comparison, it is extracted the results obtained on armour units that can be placed in a single layer such as 'Accropode®', 'Core-loc®', and 'Xbloc®' (Bruce et al., 2009).

Looking in detail at this figure, the role of the slope (3V: 4H, 2V: 3H) is obviously not negligible on the amount of overtopping. Based on the tests results, the overtopping measurement for 'Starbloc' placed on a slope of 3V: 4H following a packing density of 63% leaded to a roughness coefficient of $\gamma_r = 0.45$, given the same value for rock slope (one layer). For a 2V: 3H slope, the results deduced a roughness coefficient of about 0.40, either a decrease of about 11% compared to slope of 3V: 4H (Table 4).

Experimental tests show moderate overtopping for 'Starbloc' compared to the results of Bruce et al. (2009), with the same breakwater geometry (slope) and a closely similar packing density. However, according to the literature, it is difficult to compare two different results without taking into account the effect of different parameters such as crest width, packing density of armour layer and sub-layer, geometric characteristics of under-layers and the core and also the scale effect (Bakker et al., 2005). Nevertheless, CLASH Neural Network is a design tool to estimate wave overtopping discharges for a wide range of coastal structures. As mentioned in Van Gent et al. (2007), this method should only be used as first estimate of mean overtopping discharge.

*4.2.2. Effect of porosity on overtopping*

3D modelling software is used to place a virtual single layer of 'Starbloc' on a slope according to four different placements (Safari et al., 2012). From this modelling (autodesk), the surface porosity can be calculated inside the armour layer for several (X, Y) planes at normal elevations Z (Fig. 9-a).

The "U shaped" surface-porosity curves (Fig. 9-b) show a minimum of around 34% can occur inside the armour layer. This minimum value governs the hydraulic loss and reduces the permeability of the armour layer in favour of higher run-ups and increased under-pressure on the blocks (during the retreating wave phase).

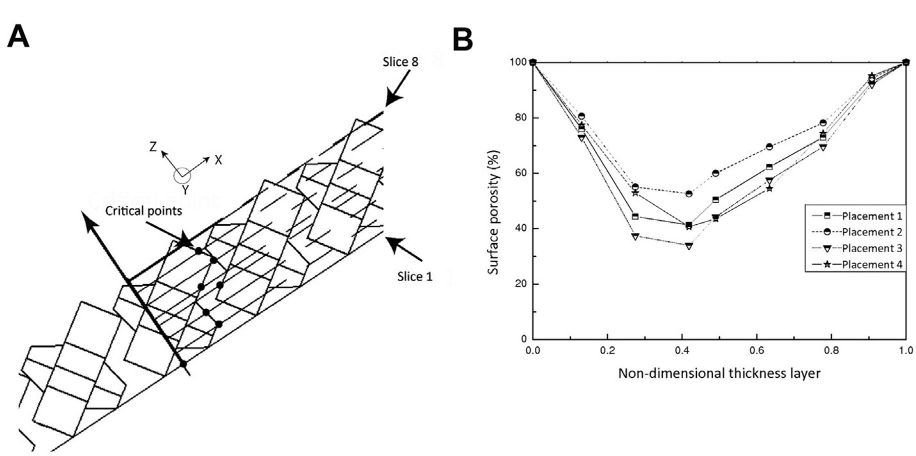


**Fig. 9.** Results of simulation models a) Schematic diagram of panel slices at critical points, b) Evaluation of surface porosity inside armour layer.

It is observed the extraction of a group of contiguous blocks in the case of placement with the lowest surface porosity. This new type of damage highlights the importance of taking into account the minimum surface porosity (instead of an overall volumetric porosity) for the design of artificial blocks on breakwaters.

## 5. Conclusion

The starbloc, a new interlocking single layer armour unit, designed for protecting sea and/or river construction works, is composed of three 'legs' and two 'noses'. The present invention is proposed to satisfy three main objectives, high hydraulic stability and performance simultaneously with easy placement.

The new block has been designed to be placed either in a random or in an orderly arrangement. Its geometry favours easy interlocking when randomly placed. Nevertheless, the various series of tests show that Starbloc® has no better stability than other available single-layer blocks ($N_s = 2.9$) for a shipshape placement. The hydraulic stability of this unit is based on its own weight and good interlocking.

The benefit in stability is balanced by somewhat lower performances in terms of overtopping ($\gamma_r = 0.45$).


## Acknowledgements

The study forms part of a research project carried out by Iman Safari under a research fellowship programme. The authors gratefully acknowledge the laboratory of Continental and Coastal Morphodynamics of the University of Caen, for the use of research facilities. The REPORTEX Company received financial support for this study.


## References


Aminti, P., Franco, L., 1988. Wave overtopping on rubble mound breakwaters. In: Proceedings of the 21th International Conference on Coastal Engineering, vol. 1, pp. 770–781.

Bakker, P., Klabbers, M., Muttray, M., van den Berge, A., 2005. Hydraulic performance of Xbloc® armour units. In: 1th International Conference on Coastal Zone Management and Engineering in the Middle East.

Bradbury, A.P., Allsop, N.W.H., Stephens, R.V., 1988. Hydraulic Performance of Breakwater Crown Walls. Report SR146, H.R. Wallingford.

Bruce, T., Van der Meer, J.W., Franco, L., Pearson, J.M., 2009. Overtopping performance of different armour units for rubble mound breakwaters. J. Coastal Eng. 56, 166–179.

Buccino, M., Calabrese, M., Ciardulli, F., Di Pace, P., Tomasicchio, G.R., 2011. One layer concrete armor units with a rock-like skin: wave reflection and run-up. J. Coast Res.

Burcharth, H.F., Liu, Z., 1994. The application of load-cell technique in the study of armour unit responses to impact loads. In: Proceedings of the 24th International Conference on Coastal Engineering, pp. 958–972.

Burcharth, H.F., Liu, Z., Troch, P., 1999. Scaling of core material in rubble mound breakwaters model test. In: Proc. of the 5th International Conference on Coastal Engineering in Developing Countries (COPEDEC), Capetown, pp. 1518–1528.

CERC, 1984. Shore protection manual [SPM], fourth ed. Coastal Engineering Research Center, US Army Corps of Engineers, Vicksburg, MS.

CIRIA, CUR, CETMEF, 2007. The Rock Manual. The Use of Rock in Hydraulic Engineering, second ed. CIRIA, London. C683.

Dupray, S., Roberts, J., 2009. Review of the use of concrete in the manufacture of concrete armour units. In: Proceeding International Conference of Coasts, Marine Structures and Breakwaters, vol. 1. ICE, Edinburgh, UK, pp. 245–259.

Edesign.co.uk, 2016. Piston coastal wave generators | Edinburgh Designs. Available at: http://www.edesign.co.uk/product/piston-wave-generators.

EurOtop, 2007. Overtopping manual, wave overtopping of sea defences and related structures: assessment manual. Pullen, T., Allsop, N. W. H., Bruce, T., Kortenhaus, A., Schüttrumpf, H., and van der Meer, J. W. www.overtopping-manual.com.

EurOtop, 2016. Manual on wave overtopping of sea defences and related structures. An overtopping manual largely based on European research, but for worldwide application. second ed. van der Meer, J.W., Allsop, N.W.H., Bruce, T., DeRouck, J., Kortenhaus, A., Pullen, T., Schüttrumpf, H., Troch, P., Zanuttigh, B., www.overtopping-manual.com.

Gómez-Martín, M.E., Medina, J.R., 2006. Damage progression on cube armored breakwaters. In: Proceedings of the 30th International Conference on Coastal Engineering, vol. 5, pp. 5229–5240.

Guo, L., Latham, J.P., Xiang, J., 2015. Numerical simulation of breakages of concrete armour units using a three-dimensional fracture model in the context of the combined finite-discrete element method. Comput. Struct. 117–142.

Hudson, R.Y., 1959. Laboratory investigation of rubble mound breakwaters. J. Waterw. Harb. Div. 93–121.

Hughes, S.A., 1993. Physical models and laboratory techniques in coastal engineering. In: Advanced Series on Ocean Engineering, vol. 7. World Scientific.

Mansard, E.P.D., Funke, E.R., 1981. The measurement of incident and reflected spectra using a least squares method. In: Proceedings of the 17th International Conference on Coastal Engineering, vol. 1, pp. 154–172.

Medina, J.R., Molines, J., Gómez-Martín, M.E., 2014. Influence of armour porosity on the hydraulic stability of cube armour layers. J. Ocean Eng. 88, 289–297.

Molines, J., Medina, J.R., 2015. Calibration of overtopping roughness factors for concrete armour units in nonbreaking conditions using the CLASH database. Coast Eng. 96, 62–70.

Möller, J., Kortenhaus, A., Oumeraci, H., De Rouck, J., Medina, J.R., 2003. Wave Run-up and Wave Overtopping on a Rubble Mound Breakwater-Comparison of Prototype and Laboratory Investigations Coastal Structures, pp. 456–468.

Owen, M.W., 1980. Design of Seawalls Allowing for Wave Overtopping. Report 924, H. R. Wallingford.

Safari, I., 2011. Analyse de la performance hydraulique d'un nouveau type de bloc artificiel utilisé pour la protection côtière. Ph. D. Thesis. University of Caen.

Safari, I., Mouazé, D., Ropert, F., Haquin, S., Ezersky, A., 2012. Influence du plan de pose sur les distributions de porosité au sein d'une carapace de digue à talus. XII[èmes] Journée Nationales Génie Côtière-Génie Civil 791–798.

Smolka, E., Zarranz, G., Medina, J.R., 2009. Estudio Experimental del Rebase de un Dique en Talud de Cubípodos. Libro de las X Jornadas Españolas de Costas y Puertos. Universidad de Cantabria-Adif Congresos, pp. 803–809 (in Spanish).

TAW, 2002. Technical Report Wave Run-up and Wave Overtopping at Dikes. Technical report. Technical Advisory Committee on Flood Defence.

USACE, 2002. In: Coastal Engineering Manual (CEM). U.S. Army Corps of Engineers, Vicksburg, Missisipi, USA.

Van Buchem, R.V., 2009. Stability of a Single Top Layer of Cubes. MSc-Thesis. Delft University of Technology, Delft.

Van der Meer, J.W., 1999. Design of concrete armour layers. In: Proc. Coastal Structures '99. A.A. Balkema, Rotterdam, pp. 213–221.

Van der Meer, J.W., Bruce, T., 2014. New physical insights and design formulas on wave overtopping at sloping and vertical structures. J. Waterw. Port, Coast. Ocean Eng. 140.

Van der Meer, J.W., Janssen, J.P.F.M., 1994. Wave Run-up and Wave Overtopping at Dikes, Delft Hydraulics No. 485.

Van der Meer, J.W., Stam, C.J.M., 1992. Wave run-up on smooth and rock slopes of coastal structures. Journal of Waterway, Port. Coastal Ocean Eng. 118, 534–550.

Van Gent, M.R.A., van den Boogaard, H.F.P., Pozueta, B., Medina, J.R., 2007. Neural network modelling of wave overtopping at coastal structures. Coast Eng. 54, 586–593.

Vandenbosch, A., Angremond, K.D., Verhagen, H.J., Olthof, J., 2002. Influence of the density of placement on the stability of armour layers on breakwaters. In: Proceedings of the 28th International Conference on Coastal Engineering. World Scientific, Singapore, pp. 1537–1549.

Vanneste, D., Troch, P., 2012. An improved calculation model for the wave induced pore pressure distribution in a rubble-mound breakwater core. Coast Eng. 66.

Victor, L., Troch, P., 2012. Experimental study on the overtopping behaviour of steep slopes - transition between mild slopes and vertical walls. In: Proceedings of the 33th International Conference on Coastal Engineering, pp. 1–23.

Wolters, G., Van Gent, M.R.A., Hofland, B., Wellens, P., 2014. Wave damping and permeability scaling in rubble mound breakwaters. In: Proc. Coastlab 2014, Varna, Bulgaria.